

A Helical Poly(amino acid) Having Carbazole Side Chains: A Candidate for a Photoelectric Liquid Crystal. 1. Synthesis and Characterization

L. L. Chapoy*

Instituttet for Kemiindustri, The Technical University of Denmark, 2800 Lyngby, Denmark

Derek Biddle

Institute of Physical Chemistry, University of Gothenburg and Chalmers University of Technology, 412 96 Gothenburg, Sweden

J. Halstrøm, K. Kovács, K. Brunfeldt, M. A. Qasim, and T. Christensen

The Danish Institute of Protein Chemistry, 2970 Hørsholm, Denmark.

Received April 27, 1982

ABSTRACT: A novel poly(α -amino acid) having carbazole pendant groups has been synthesized and characterized. The resulting polymer has been shown to be a high molecular weight material in the α -helical conformation. A cholesteric lyotropic mesophase was formed in concentrated solution. The significance of long-range liquid crystalline order for photoconductivity is discussed.

Introduction

In recent years, there has been intense interest in the synthesis and study of carbazole-containing polymers. Such polymers are known to be both photovoltaic¹ and photoconductive,² desirable properties that could lead to a number of interesting engineering applications. The photophysics of these polymers thus occupies a central place in regard to the development of new materials with these desirable photoresponsive properties.

There are numerous indications that such electronic transport phenomena are sensitive to the geometrical arrangement of the active groups and hence would be enhanced by a polymer possessing long-range molecular order, analogous to the stacking behavior of one-dimensional organic conductors.³ Recently, the mechanical orientation of polyacetylene⁴ as well as the preparation of poly(*p*-phenylene) single crystals⁵ from crystalline oligomers has resulted in considerably enhanced conductivity.

In the area of photoactive materials there is a strong spatial dependence for both the nonradiative energy transfer of the excited state^{6,7} (Förster mechanism) and the formation of excimer traps⁸ leading to nonlinear emission from the monoexcited dimer. Nonradiative energy transfer is a long-range oscillator coupling of chromophores taking place over distances the order of 100 Å, while excimer formation is a short-range effect, i.e., a type of bonding interaction occurring over distances of 1.5 to perhaps 6 Å. The coupling of neighboring chromophores as evidenced by excimer formation is thought to be a precursor to photoconductive behavior.⁹

In addition, interesting photovoltaic behavior has been demonstrated by suitably doped lipid bilayers having a smectic liquid crystalline structure¹⁰ as well as by chlorophyll-doped nematic liquid crystals intended to model the photosynthetic process,¹¹ for which the *in vivo* ordering of chlorophyll is thought to be an intrinsic feature.

The dependence of such electrical properties on orientation could, however, alternatively be postulated *a priori* based on the inherent anisotropy of the π orbitals in the active chromophore.

With this in mind, we have synthesized and characterized a liquid crystal forming polymer having pendant carbazole groups so that the effect of order on the photoconductive and photovoltaic behavior as well as the photophysics of excimer formation could be investigated. More specifically, a polylysine derivative, poly[*N*-(9-carbazolylcarbonyl)-L-lysine] (PKL), i.e., a poly(amino acid)

having the structure shown in Figure 1, was prepared from the corresponding *N*-carboxyanhydride (NCA). Such poly(amino acid) polymers are generally known to have helical conformations and to form lyotropic mesophases in concentrated solution.¹² This requires, however, that the molecular weight is high enough to obtain a sufficient aspect ratio of the resulting helix as required by the Flory theory.¹³ In addition the necessary helical conformation will only form if the optically active NCA does not racemize during polymerization.

The photoconductivity of a carbazole derivative of poly(glutamic acid) has been studied,¹⁴ but no mention was made of either the molecular weight or the propensity of the material used to form the liquid crystalline phase. The effect of the morphology on the electrical properties was not investigated.

Synthesis

The carbazole-substituted NCA shown in Figure 1 is readily prepared by the following procedure: (1) The amino acid-Cu(II) complex is reacted with 9-(chlorocarbonyl)carbazole¹⁵ in aqueous bicarbonate/acetone solution to form the copper complex of *N*-(9-carbazolylcarbonyl)lysine. Note that the use of the copper complex automatically ensures reaction with the desired amine group. (2) The copper complex is destroyed by treatment with formic acid, and the pure lysine derivative is precipitated by diluting the filtrate with water. (3) The NCA is formed by reacting a tetrahydrofuran suspension of the amino acid with phosgene. Both the amino acid and the NCA were optically active.¹⁶

The dry NCA was stable for months but polymerized readily at room temperature when dissolved in dioxane on initiation with methanolic sodium hydroxide. High molecular weight polymer was obtained by adding a slight excess of initiator relative to that required to titrate the small amount of impurities present. Additional initiator depressed the molecular weight as expected from the polymerization mechanism. When all the NCA had reacted, as indicated by thin layer chromatography, the polymer was isolated after precipitation by the dropwise addition of the viscous solution to ethanol.

Sample Characterization

A. Molecular Weight. Since PKL was readily soluble in tetrahydrofuran (THF) polymerization conditions could be optimized with respect to the preparation of high molecular weight samples by the use of a standard gel permeation chromatograph. It was not possible by this procedure to determine the absolute molecular weight directly since Mark-Houwink parameters are not available for this novel polymer, and the expected helical conformation

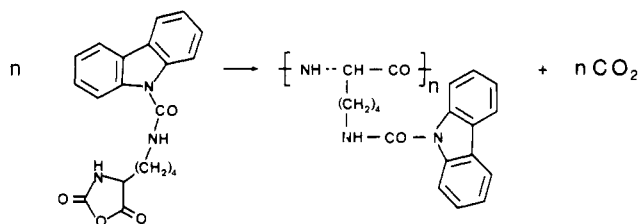


Figure 1. Formation of poly[N-(9-carbazolylcarbonyl)-L-lysine] (PKL) from the corresponding *N*-carboxyanhydride.

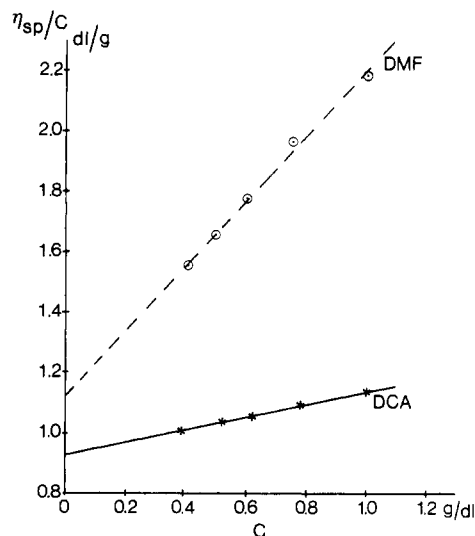


Figure 2. Intrinsic viscosity data for a high molecular weight sample of poly[N-(9-carbazolylcarbonyl)-L-lysine] (PKL) in DMF and DCA.

made use of the universal calibration procedure problematic.

The intrinsic viscosity was measured in dimethylformamide (DMF) and dichloroacetic acid (DCA) at 25 °C. DMF is known to be a heliogenic nonaggregating solvent, while DCA is known to be a denaturing solvent for similar polymers.¹⁷ The intrinsic viscosity data for a high molecular weight sample that was used exclusively in the remaining studies and a low molecular weight sample are shown in Figures 2 and 3, respectively. The Mark-Houwink equation $[\eta] = KM_v^a$, where $[\eta]$ is the intrinsic viscosity and M_v the viscosity-average molecular weight, is given as follows for poly(γ -benzyl L-glutamate) (PBLG):¹⁸ (1) DMF, $K = 2.9 \times 10^{-9}$, $a = 1.70$; (2) DCA, $K = 2.78 \times 10^{-5}$, $a = 0.87$. Note that the smaller coefficient K and larger exponent a for the case of the helical DMF solutions dictate that for large M_v , $[\eta]$ will be larger for the helix than the denatured coil, while the reverse will be true at lower molecular weights. This is indeed the case for the data presented in Figures 2 and 3 as well as for data previously reported for PBLG.¹⁷ An attempt was made to crudely estimate the molecular weight for the PKL based on the Mark-Houwink equation for PBLG corrected by the ratio of the molecular weight per repeat unit, a kind of universal calibration for α -helical poly(amino acids). This procedure gave for the high molecular weight sample in Figure 2 an $M_v = 1.13 \times 10^5$ in DMF and 1.59×10^5 in DCA.

The absolute determination of the molecular weight was achieved by the use of a Chromatix KMX-6 small-angle light scattering apparatus coupled on-line to a gel permeation chromatograph (GPC). Simultaneous measurements of the Rayleigh scattering at 632.8 nm and the differential refractive index of the eluted polymer in THF solutions were recorded. The Rayleigh scattering provides the molecular weight information while the differential

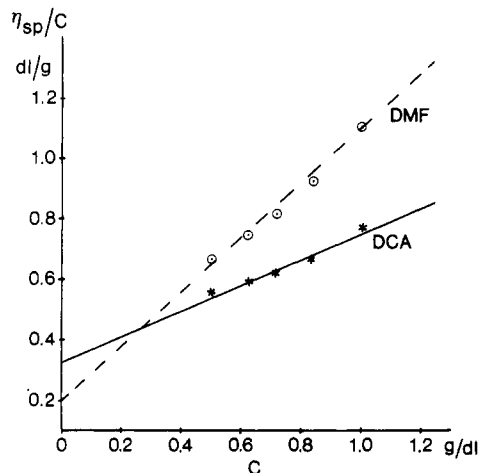


Figure 3. Plot as in Figure 2 for low molecular weight sample.

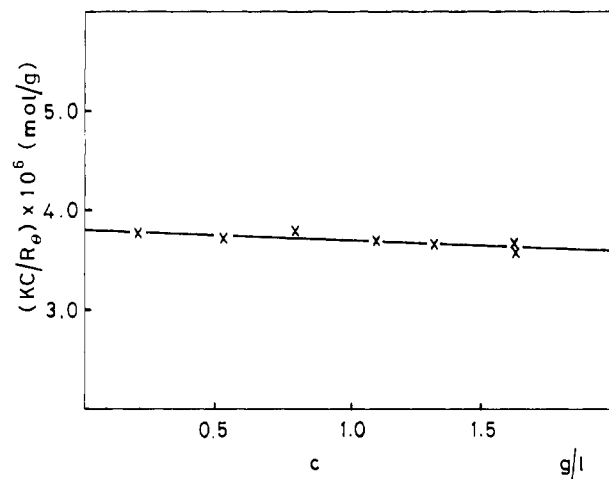


Figure 4. Standard light scattering plot showing the reduced scattering intensity as a function of concentration. The reciprocal of the intercept is M_w .

refractive index provides the concentration information as the polymer is continuously fractionated by the GPC. These two curves plus the concentration gradient of the refractive index dn/dc and the second virial coefficient (A_2) obtained from static small-angle light scattering measurements as a function of concentration enable one to construct the molecular weight distribution. A_2 and dn/dc determinations were performed on the whole polymer and were assumed to be molecular weight independent. dn/dc was determined on a Shimadzu DR-4 differential refractometer at 546 and 578 nm at 25 °C giving dn/dc values of 0.224 and 0.220, respectively. From these data, dn/dc at 632.8 nm was extrapolated to be 0.213. The static results, shown in Figure 4, yielded $M_w = 2.63 \times 10^5$. Note that THF is approximately a θ solvent for this polymer. Note that these results are within a factor of 2 of those results obtained by the already-mentioned intrinsic viscosity procedure and the latter thus could be useful for an initial screening of reaction conditions for newly synthesized poly(amino acids).

The light scattering data for the GPC fractionated polymer are shown in Figure 5. The two curves represent the differential refractive index and the light scattering signals arising from the eluted solutions. Note as expected the intense scattering at short times, i.e., low elution volumes and high molecular weight material, where the concentration is still low. The small vertical lines in Figure 5 indicate equivalent elution volumes. This shift arises from using series-connected flow cells and a two-channel

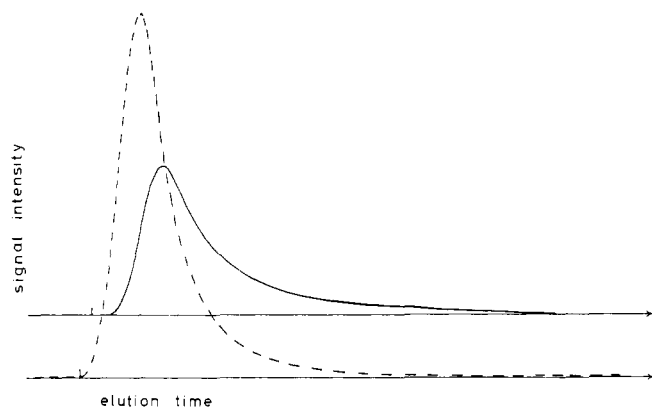


Figure 5. Two-detector gel permeation chromatogram showing signal intensity as a function of elution time. The dashed line is the light scattering intensity and the solid line is the differential refractive index. The small vertical lines indicate equivalent elution volume.

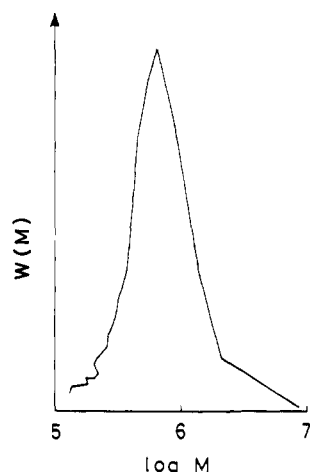


Figure 6. Molecular weight distribution as calculated from the data in Figure 5. $W(M)$ is the weight fraction of polymer having molecular weight M .

recorder. The calculated molecular weight distribution is shown in Figure 6 and yields computed molecular weight averages $M_n = 4.04 \times 10^5$ and $M_w = 5.66 \times 10^5$. Note that M_w as obtained in this way is appreciably higher than that obtained for the whole polymer. We ascribe this discrepancy to the pronounced low molecular weight tail as evidenced by the differential refractive index data. Since this low molecular weight tail gives rise to almost no scattering, the molecular weight distribution curve must be very imprecise or nonexistent in the low molecular region, giving anomalously high values of both M_n and M_w . Due care must be exercised in the case of unfavorable molecular weight distributions when the above-mentioned instrumental techniques are used.

B. Conformational Studies. The evidence for the existence of the helical structure in dilute solution is given by the infrared (IR) spectrum and the circular dichroic (CD) behavior of the PKL.

The CD was studied in the region 210–340 nm in dilute dioxane solution. Dioxane is also known to be a helicogenic solvent. Spectra were recorded on a Cary 60 spectropolarimeter equipped with a 6002 CD accessory, calibrated at 304 nm with dioxane (spectroscopic quality) solutions of androsterone. Data were obtained in a 1-mm cell and are reproduced in Figure 7.

Polylysine is known to exist in the helical form and its CD has been extensively studied as a model for the use of CD in the evaluation of protein structure.¹⁹ In the region

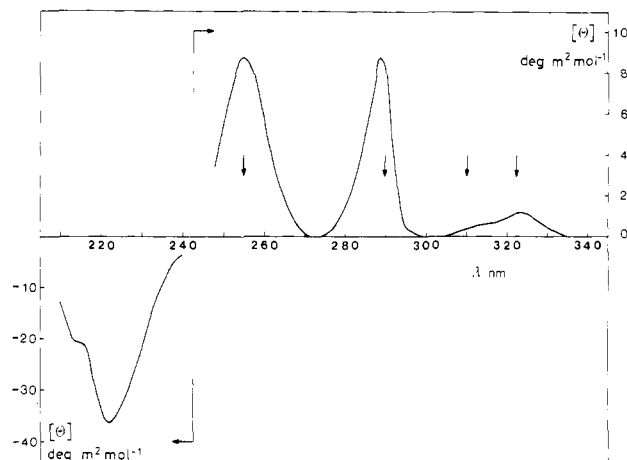


Figure 7. Circular dichroic spectrum of poly[*N*-(9-carbazolyl-carbonyl)-L-lysine] (PKL) in dioxane. The concentrations have been adjusted to give an absorbance of ca. 1. In the wavelength range 210–240 nm, the concentration was 3.18×10^{-4} M with respect to monomer and 3.18×10^{-3} M in the range 245–340 nm. $1 \text{ deg m}^2 \text{ mol}^{-1} = 10^3 \text{ deg cm}^2 \text{ dmol}^{-1}$.

around 220 nm distinctive spectra are observed for the random coil, β , and α -helix structures, and the observed CD can be used to estimate the helical content in nonuniform structures. Greenfield and Fasman¹⁹ report a molar ellipticity of about $-35 \text{ deg m}^2 \text{ mol}^{-1}$ at 222 nm, and similar values are reported in numerous other papers.²⁰ For the water-insoluble poly(*N*-carbobenzoxylysine) in hexafluoro-2-propanol a value of $-29 \text{ deg m}^2 \text{ mol}^{-1}$ is reported.²¹ We observed $-36 \text{ deg m}^2 \text{ mol}^{-1}$ for our carbazole-substituted polymer in dioxane, which would suggest a high degree of helicity. However, Yoshikawa et al.²² reported the molar ellipticity of the 222-nm band of poly[γ -[2-(9-carbazolyl)ethyl] L-glutamate] (PKG) as $45.4 \text{ deg m}^2 \text{ mol}^{-1}$, an unusually high value, which may or may not be due to the carbazolyl side group.

Above 250 nm we observe the expected induced CD of the carbazole chromophore, with peaks corresponding to bands observed in the absorption spectrum (marked by arrows). However, in contrast to solution CD spectra of PKG, the spectrum of our polymer exhibits only positive CD in this region and thus resembles very closely the spectra obtained for solid films of PKG,²² with regard to both spectral form and intensity. This would indicate significant differences in side-chain conformation for PKL and PKG in solution. Since the side-chain peaks are considerably more intense in PKL, we conclude that the side chains are more oriented with respect to the helical backbone than in PKG. We hope to make a more detailed study of the induced carbazole CD in the near future since valuable information regarding side-group orientation with respect to the helix should be available from such studies.

Conformational information is also available from IR spectroscopy. The α helix shows characteristic absorption bands at 1650 cm^{-1} and 1550 cm^{-1} whereas the β -structure absorption is shifted to lower frequencies.²³ The IR spectrum of PKL in dioxane recorded on a Nicolet MX-1 Fourier transform spectrometer and shown in Figure 8 clearly indicates the helical structure of PKL.

Liquid Crystalline Behavior

Concentrated solutions of PKL in THF spontaneously formed what appeared to be a cholesteric lyotropic mesophase with its characteristic fingerprint pattern when viewed between crossed polarizers as shown in Figures 9 and 10. This is a well-known feature of poly(amino acids) and again is supportive of the rigid helical conforma-

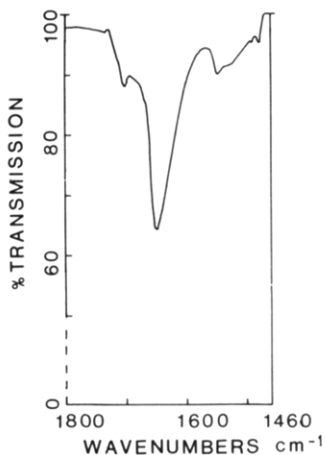


Figure 8. Infrared spectrum of poly[*N'*-(9-carbazolylcarbonyl)-L-lysine] (PKL) in dioxane in the frequency range 1800–1450 cm^{-1} showing the characteristic α -helical amide I and amide II bands at 1550 and 1650 cm^{-1} .

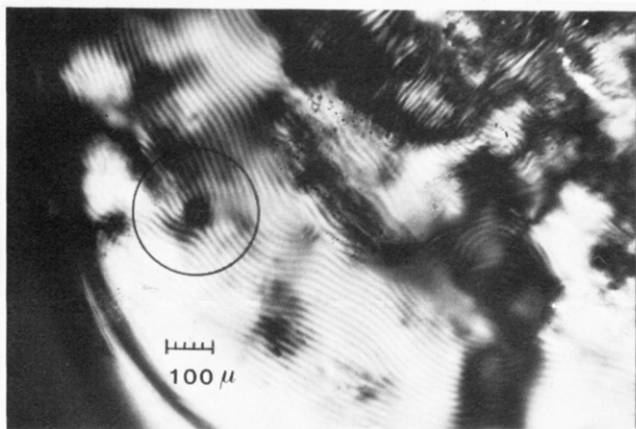


Figure 9. Light micrographs of a 23% solution of poly[*N'*-(9-carbazolylcarbonyl)-L-lysine] (PKL) in tetrahydrofuran viewed between crossed polars showing the fingerprint pattern characteristic of the cholesteric mesophase.

tion.^{12,24} The black lines are due to the cholesteric pitch periodically bringing the principal axes of the molecules parallel to one of the axes of the polarizers in the laboratory coordinate system. The line spacing is thus a direct measure of the cholesteric twisting power of the system, i.e., the distance required for a twist of 90°. Figures 9 and 10 show the structure present at ca. 23% concentration in THF in a standard 1-mm path length cuvette. The determination of the critical concentration for the onset of mesophase formation was obscured by a slow development of the fingerprint pattern after stirring or pouring. Most line spacings are between 15 and 20 μm as might be expected.²⁴ Note the defect structure in the form of a $+\pi, -\pi$ disclination dipole as indicated in Figure 9. Note also the appreciable parallel wall orientation in Figure 10, extending almost 0.5 mm in from the edge. Such surface orientations, capable of propagating over macroscopic distances, are well-known phenomena in liquid crystals. Uematsu et al. in recent interesting studies of such surface effects have proposed an interaction between the dipoles on the glass surface, with the chain dipoles serving to promote surface alignment.²⁵ No thermal transitions were observed by differential scanning calorimetry at temperatures up to 200 °C, precluding thermotropic behavior in this temperature range.

Since the absorption and emission oscillators are thought to reside in the carbazole ring plane, effective photoconductive enhancement employing a polymer such as in-

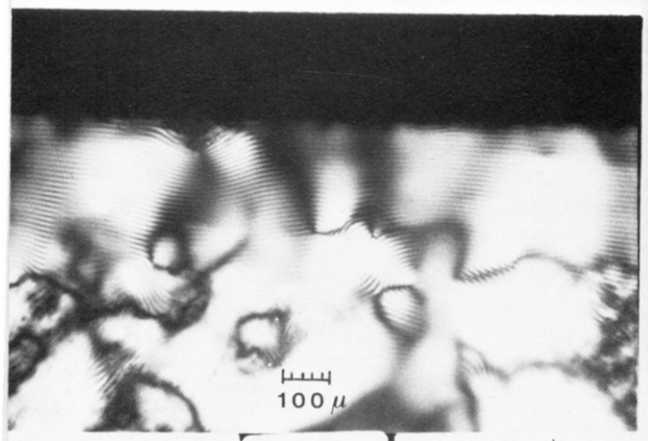


Figure 10. As in Figure 9.

vestigated in this study would, however, require homeotropic, nematic alignment to promote the macroscopic stacking of the carbazole substituents in the sample plane. Recent suggestions have been made as to how this morphology might be attained.^{25,26}

Additional studies are in progress with regard to the photophysics, control of the sample morphology, and the photoelectric properties.

Acknowledgment. We thank Knud Rasmussen, Renny Gilsager, and Anne Trojaborg for help with the measurements, especially the photographic work. The help of Vagn Handlos from the Royal Danish School of Pharmacy in obtaining the small-angle light scattering data is also appreciated. L.L.C. and the group from the Danish Institute of Protein Chemistry acknowledge financial support from Statens Tekniske Videnskabelige Forskningsråd. D.B. acknowledges the financial support of the Swedish Natural Science Research Council.

Registry No. PKL (repeating unit), 84117-59-9; PKL (homopolymer), 84110-21-4; PKL NCA (homopolymer), 84117-61-3.

References and Notes

- Hoegl, H. *J. Phys. Chem.* **1965**, *69* (3), 755.
- Reucroft, P. J.; Takahashi, K.; Ullal, H. *J. Appl. Phys.* **1975**, *46* (12), 5218.
- Dirk, C. W.; Schoch, K. F.; Marks, T. J. "Conductive Polymers"; Seymour, R. B., Ed.; Plenum Press: New York, 1981; pp 209ff.
- Park, Y.; Druy, M. A.; Chiang, C. K.; MacDiarmid, A. G.; Heeger, A. J.; Shirakawa, H.; Ikeda, S. *J. Polym. Sci., Polym. Lett. Ed.* **1979**, *17*, 195.
- Shacklette, L. W.; Eckhardt, H.; Chance, R. R.; Miller, G. G.; Ivory, D. M.; Baughman, R. H. Reference 3, pp 115ff.
- Weber, G. *Trans. Faraday Soc.* **1954**, *50*, 552.
- Chapoy, L. L.; Spaseska, D.; Rasmussen, K.; DuPré, D. B. *Macromolecules* **1979**, *12*, 680.
- Birks, J. B. In "The Exciplex"; Gordon, M.; Ware, W. R., Eds.; Academic Press: New York, 1975; pp 39ff.
- Slobodyanik, V. V.; Naidyonov, V. P.; Pochinok, V. Ya.; Yashchuk, V. N. *Chem. Phys. Lett.* **1981**, *81*, 582.
- Tien, H. Ti. *Nature (London)* **1970**, *227*, 1232.
- Aizawa, M.; Hirano, M.; Suzuki, S. *Electrochim. Acta* **1978**, *23*, 1185.
- Robinson, C. *Trans. Faraday Soc.* **1956**, *52*, 571.
- Flory, P. J. *Proc. R. Soc. London, Ser. A* **1956**, *234*, 73.
- Tanikawa, K.; Okuno, Z.; Iwaoka, T.; Hatano, M. *Makromol. Chem.* **1977**, *178*, 1779.
- Ruigh, W. L. U.S. Patent 2 089 985, 1937.
- Halström, J.; Chapoy, L. L.; Kovács, K.; Brunfeldt, K.; Qasim, M. A. *Pept., Proc. Eur. Pept. Symp., 16th, 1980* **1981**, 759–67.
- Doty, P.; Bradbury, J. H.; Holtzer, A. M. *J. Am. Chem. Soc.* **1956**, *78*, 947.
- Brandrup, J.; Immergut, E. H., Eds. "Polymer Handbook"; Interscience: New York, 1966.
- Greenfield, N.; Fasman, G. D. *Biochemistry* **1969**, *8*, 4109.
- Woody, R. W. *J. Polym. Sci., Macromol. Rev.* **1977**, *12*, 223.
- Parrish, J. R.; Blout, E. R. *Biopolymers* **1971**, *10*, 1491.

- (22) Yoshikawa, M.; Nomori, H.; Hatano, M. *Makromol. Chem.* **1978**, *179*, 2397.
- (23) Ambrose, E. J.; Hanby, W. E. *Nature (London)* **1949**, *163*, 483.
 Elliot, A.; Ambrose, E. J. *Ibid.* **1950**, *165*, 921. Beer, M.; Sutherland, G. B. B. M.; Tanner, K. N.; Wood, D. L. *Proc. R. Soc. London, Ser. A* **1959**, *249*, 147.
- (24) Robinson, C.; Ward, J. C.; Beevers, R. B. *Discuss. Faraday Soc.* **1958**, *25*, 29.
- (25) Uematsu, Y.; Tomizawa, J.; Kidokoro, F.; Sasaki, T. *Annu. Rep. Tokyo Inst. Polytechnics* **1980**, *2*, 53.
- (26) Fernandes, J. R.; DuPré, D. B. *Mol. Cryst. Liq. Cryst.* **1981**, *72*, 67.

Triple Helix of *Schizophyllum commune* Polysaccharide in Dilute Solution. 5. Light Scattering and Refractometry in Mixtures of Water and Dimethyl Sulfoxide

Takahiro Sato, Takashi Norisuye,* and Hiroshi Fujita

Department of Macromolecular Science, Osaka University, Toyonaka, Osaka 560, Japan.

Received April 23, 1982

ABSTRACT: Light scattering and differential refractive index measurements were made on a sonicated sample of schizophyllan in water + dimethyl sulfoxide (Me_2SO) mixtures over the entire composition range at 25 °C. When the water composition was diminished to about 13 wt %, the weight-average molecular weight M_w and the z-average mean-square radius of gyration $\langle S^2 \rangle_z$ were found to decrease abruptly to the values in pure Me_2SO . This result directly checks the previous deduction from viscosity data that the triple helix of schizophyllan would dissociate to single randomly coiled chains at a water composition of about 13 wt %. Analysis of the M_w and $\langle S^2 \rangle_z$ data indicated that the dissociation proceeds in all-or-none fashion. Specific refractive index increments for dialyzed and undialyzed solutions showed that the Me_2SO molecule adsorbs preferentially on schizophyllan in the region of water composition below about 40 wt %.

Schizophyllan is an extracellular polysaccharide consisting of linearly linked β -1,3-D-glucose residues with one β -1,6-D-glucose side chain for every three main-chain residues.^{1,2} In part 1,³ we found that this polysaccharide dissolves in water as a rodlike triple helix, while it disperses in dimethyl sulfoxide (Me_2SO) as a single randomly coiled chain. We also found that the intrinsic viscosity $[\eta]$ of schizophyllan in mixtures of water and Me_2SO at 25 °C undergoes an almost discontinuous decrease when the water composition is decreased to about 13 wt %. This decrease in $[\eta]$ was taken as reflecting a sharp dissociation of the triple helix to single chains.

In part 2,⁴ we explored thermal effects on the schizophyllan triple helix in the water + Me_2SO mixture at a water composition of 12.76 wt % by viscometry and ultracentrifugation. When the solution was heated, for example, at 30 °C, $[\eta]$ decreased slowly with time and virtually leveled off at a constant after about 24 h. Schlieren patterns for this final solution revealed the presence of the triple helix and the single chain but not any other species. When the solution was examined at a higher temperature of 45 °C, the schlieren peak corresponding to the triple helix disappeared and $[\eta]$ approached the value in pure Me_2SO . From these results we concluded that the schizophyllan triple helix melts into single chains in all-or-none fashion with increasing temperature.

This paper reports a light scattering study undertaken to see whether the isothermal solvent-induced dissociation of the schizophyllan triple helix in water + Me_2SO mixtures also proceeds in all-or-none fashion.

Experimental Section

Preparation of Solutions. A purified, sonicated fraction of schizophyllan chosen from our stock was used for all measurements. A weighed amount of the sample was dissolved in the water + Me_2SO mixture of a desired composition at a temperature below 25 °C, and the solution was left standing at 25 °C for 1 day. By diluting it with the same mixed solvent of 25 °C, we prepared a series of polymer concentrations.

Dimethyl sulfoxide was dehydrated with calcium hydrate and fractionally distilled in a reduced nitrogen atmosphere. Densities ρ_0 and refractive indices n_0 of water + Me_2SO mixtures at 25 °C were evaluated by interpolating or extrapolating the reported values⁵ and our previously measured values.

Differential Refractometry. We constructed a dialyzer so designed that both the solution and solvent compartments can be stirred; their capacities were about 8 and 50 cm³, respectively. The solution was separated from the mixed solvent by a Visking gel-cellophane membrane, and the entire system was thermostated at 25 ± 0.1 °C. Before setting, the membrane was conditioned by washing it successively with 0.01 N acetic acid, water, and the mixed solvent. Osmotic equilibrium was attained after 2-4 days.

Specific refractive index increments $(\partial n/\partial c)_{T,\mu}$ for dialyzed solutions and $(\partial n/\partial c)_{T,p,w_H}$ for undialyzed ones, both at 25 °C, were determined by using a differential refractometer of the modified Schulz-Cantow type calibrated with Kruis' data⁶ on aqueous potassium chloride. Here, T and p have the usual meaning, and μ and w_H denote the chemical potentials of the diffusible components (i.e., water and Me_2SO) in the solution and the weight fraction of water in the mixed solvent, respectively. In the subsequent presentation, the subscripts T and p are omitted for simplicity.

Refractive index increments $(\partial n_0/\partial w_H)$ of water + Me_2SO mixtures at 25 °C were evaluated from the slope of n_0 vs. w_H or directly measured in the differential refractometer.

Light Scattering. Intensities scattered from schizophyllan solutions in water + Me_2SO mixtures at 25 °C were measured on a Fica 50 automatic light scattering photometer in an angular range from 22.5 to 150°. Instead of pure water solutions those containing 0.01 N sodium hydroxide (NaOH) were used, for the reason mentioned in part 4.⁷ Vertically polarized incident light of 546-nm wavelength was used for most of the measurements. The photometer was calibrated in the same way as described previously.⁷

Solutions of $w_H = 0.1270$ and 0.1000 were investigated at a fixed scattering angle of 90° with an analyzer set in the vertical direction or the horizontal direction. The scattering intensity I_H , relative to I_{V_0} was found to be virtually zero for any of the solutions, where I_H and I_{V_0} denote the intensities measured for vertically polarized incident light with the analyzer oriented in the horizontal direction and the vertical direction, respectively. Thus, the optical an-